Appl. Math. Mech. -Engl. Ed., **35**(6), 729–740 (2014)
DOI 10.1007/s10483-014-1825-6

Applied Mathematics and Mechanics (English Edition)

Numerical well test for well with finite conductivity vertical fracture in coalbed*

Yue-wu LIU (刘曰武)[1], Wei-ping OU-YANG (欧阳伟平)[1], Pei-hua ZHAO (赵培华)[2], Qian LU (鹿 倩)[2], Hui-jun FANG (方惠军)[3]

(1. Institute of Mechanics, Chinese Academy of Sciences, Beijing 100190, P. R. China;
2. PetroChina Coalbed Methane Company Limited, Beijing 100028, P. R. China;
3. Well Test Department of Geermu Oil Factory of Qinghai Oil Field, Geermu 816000, Qinghai Province, P. R. China)

Abstract A new well test model is developed for the hydraulic fractured well in coalbed by considering the following aspects: methane desorption phenomena, finite conductivity vertical fractures, and asymmetry of the fracture about the well. A new parameter is introduced to describe the storage of the fracture, which is named as a combined fracture storage. Another new concept called the fracture asymmetry coefficient is used to define the asymmetry of the fracture about the well. Finite element method (FEM) is used to solve the new mathematical model. The well test type curves and pressure fields are obtained and analyzed. The effects of the combined fracture storage, desorption factor, fracture conductivity, and fracture asymmetry coefficient on the well test type curves are discussed in detail. In order to verify the new model, a set of field well test data is analyzed.

Key words coalbed, fractured well, numerical method, finite element method (FEM), finite conductivity

Chinese Library Classification O242.21, O346.1, TD821
2010 Mathematics Subject Classification 74S05, 74A45

1 Introduction

Coalbed methane (CBM) is one of the most important gas resources developed recently in China. The permeability of coalbed in China is generally very low. The productivity of low permeability coalbed is poor, which makes the production rate of water and gas to be very slow. In order to improve the productivity of wells in coalbed, the hydraulic fracturing technology is used in most of the CBM wells in China. A fracture through the wellbore is formed after the hydraulic fractures. The fracture can reduce the flow resistance near the wellbore. Assessing the characters of the fracture and the coalbed from well test data is an especial key step for a reasonable producing process.

A great number of studies have been published in the literature on hydraulic fractured wells. However, most of the published well testing models are analytical models, and only a few

* Received Jul. 21, 2013 / Revised Oct. 15, 2013
Project supported by the National Science and Technology Major Project of China (No. 2011ZX05038-003) and the Science and Technology Project of PetroChina Company Limited (No. 2010E-2205)
Corresponding author Yue-wu LIU, Professor, Ph. D., E-mail: lywu@imech.ac.cn

numerical models have been presented. The analytical models are based on many assumptions. There are many methods to develop fracture well test models. Gringarten et al.[1] developed a well test model for the vertical fractured well in a normal reservoir by using the source and Green's functions. They assumed that the fracture was a uniform flux fracture or an infinite conductivity fracture. Cinco-Ley and Meng[2] and Cinco-Ley and Samaniego[3] introduced a more general well test model for the fractured well with a finite conductivity vertical fracture. Lee and Brockenbrough[4] developed a fractured well model by assuming the trilinear flow near a finite conductivity fracture. Riley et al.[5] presented exact analytic solutions for an elliptical finite conductivity fracture. Liu and Yang[6] and Liu and Liu[7] developed an elliptical flow model for a finite conductivity fractured well. Anbarci and Ertekin[8] developed a uniform-flux vertical fracture model in consideration of the unsteady-state sorption phenomena in coalbed. He and Hang[9] found a model to assess a new finite conductivity fractured well by considering the deformation of media in coalbed. Liu et al.[10] developed a numerical model for the multiwell in coalbed. The above results of CBM wells are all derived from the pseudo-steady state desorption model[11] or unsteady state desorption model[12] by using the Langmuir adsorption theory[13]. In 2010, Ouyang and Liu[14] developed a new model for a fractured well in coalbed with an infinite conductivity fracture by considering the steady state desorption. The advantage of the numerical approach is that it is based on fewer assumptions than analytic solutions, and hence has greater generality. In this paper, based on the above published works, a new numerical well test model for a fractured well with a finite conductivity vertical fracture is presented.

The main aspects considered in the model are as follows:

(i) The desorption phenomenon[15] is one of the key features between normal gas and coalbed methane in the producing process, and the effects of the steady and unsteady terms of desorption are dealt within the model.

(ii) The hydraulic fracture is vertical.

(iii) More stuffs make lower conductivity fractures as finite vertical fractures.

(iv) The asymmetry of the fracture is around the axis of the well.

Since the governing equation and the inner boundary condition in the coalbed are very complex, finite element method (FEM) is used to solve the new mathematical model. The effects of the desorption factor, size, and permeability of the damage region, fracture length, asymmetry coefficient on the type curve are all discussed in detail in this paper. In order to verify the new model, a set of field well test data is analyzed.

2 Physical and mathematical models

2.1 Physical model

a) The media is homogenous in the coalbed.

b) The fluid in the coalbed is compressible and Newtonian with constant viscosity.

c) The fluid flow in the coalbed is laminar, and obeys the Darcy theorem. The model considers the wellbore boundary and the flux of wellbore boundary.

d) The manufactured fracture is vertical with certain permeability and width. The value of permeability in the fracture is greatly larger than that of the coalbed. There is a pressure difference in the fracture. The wellbore is not uniform, but the pressure at each point of the wellbore is assumed to be equal.

e) The desorption values of the CBM are linear with pressure, and are independent of time during the test processing.

f) The saturation of water within the coalbed is very low, or the distribution of saturation of water is stable and almost irreducible. Only coal gas is considered in the coalbed. Water affects the permeability of gas there.

g) The changes of gravity and temperature are neglected, and other physical and chemical effects are also ignored.

2.2 Mathematical model

The governing equation is

$$\frac{\partial^2 p_{\mathrm{D}}}{\partial x_{\mathrm{D}}^2}+\frac{\partial^2 p_{\mathrm{D}}}{\partial y_{\mathrm{D}}^2}+\alpha_{1\mathrm{D}}+\alpha_{2\mathrm{D}}(p_{\mathrm{D}}-p_{\mathrm{CD}})$$
$$=\frac{1}{C_{\mathrm{fD}}K_{\mathrm{r}}}\frac{\partial p_{\mathrm{D}}}{\partial T_{\mathrm{D}}},\quad x_{\mathrm{D}},y_{\mathrm{D}}\in\Omega. \tag{1}$$

The initial condition is

$$p_{\mathrm{D}}=0. \tag{2}$$

The inner boundary condition is

$$\sum_{i=1}^{N}L_{i\mathrm{D}}\Big(\frac{\partial p_{i\mathrm{D}}}{\partial n}\Big)\Big|_{\Gamma_{\mathrm{in}}}=2\pi\Big(1-\frac{\mathrm{d}p_{\mathrm{wD}}}{\mathrm{d}T_{\mathrm{D}}}\Big), \tag{3}$$

$$p_{i\mathrm{D}}=p_{\mathrm{wD}}. \tag{4}$$

The infinite outer boundary is

$$p_{\mathrm{D}}|_{x,y\to\infty}=0. \tag{5}$$

The constant outer pressure boundary is

$$p_{\mathrm{D}}|_{\Gamma_{\mathrm{out}}}=0. \tag{6}$$

The closed outer boundary is

$$\frac{\partial p_{\mathrm{D}}}{\partial n}\Big|_{\Gamma_{\mathrm{out}}}=0. \tag{7}$$

In the above equations, p_{D} is the dimensionless pressure, T_{D} is the dimensionless time, $(x_{\mathrm{D}},y_{\mathrm{D}})$ is the dimensionless position in the coalbed, p_{CD} is the dimensionless critical desorption pressure[16], $\alpha_{1\mathrm{D}}$ is the dimensionless steady desorption coefficient, $\alpha_{2\mathrm{D}}$ is the dimensionless unsteady desorption coefficient, K_{r} is the ratio of fracture permeability to coalbed permeability, $L_{i\mathrm{D}}$ is the dimensionless inner boundary length of the ith element, p_{wD} is the dimensionless wellbore pressure, $p_{i\mathrm{D}}$ is the dimensionless pressure of the ith element, Γ_{in} indicates the inner boundary, Γ_{out} indicates the outer boundary, Ω indicates the research region, and C_{fD} is the dimensionless combined fracture storage.

2.3 Calculating methods

2.3.1 FEM method

To solve the above mathematical model, the Galerkin finite element method with the weighted residual method is used, and the selected interpolation function N_i is used as the weight function, where

$$N_i=a_i+b_ix_{\mathrm{D}}+c_iy_{\mathrm{D}},\quad i=1,2,3.$$

Then,

$$\iint_A N_i^e\Big(\frac{\partial^2 p_{\mathrm{D}}}{\partial x_{\mathrm{D}}^2}+\frac{\partial^2 p_{\mathrm{D}}}{\partial y_{\mathrm{D}}^2}+\alpha_{1\mathrm{D}}+\alpha_{2\mathrm{D}}(p_{\mathrm{D}}-p_{\mathrm{CD}})$$
$$-\frac{1}{C_{\mathrm{fD}}K_{\mathrm{r}}}\frac{\partial p_{\mathrm{D}}}{\partial T_{\mathrm{D}}}\Big)\mathrm{d}A=0. \tag{8}$$

The weak solution formation is

$$\iint_A \Big(\frac{\partial N_i^e}{\partial x_{\rm D}}\frac{\partial p_{\rm D}}{\partial x_{\rm D}} + \frac{\partial N_i^e}{\partial y_{\rm D}}\frac{\partial p_{\rm D}}{\partial y_{\rm D}} - N_i^e(\alpha_{1\rm D} + \alpha_{2\rm D}(p_{\rm D} - p_{\rm CD})) + \frac{N_i^e}{C_{\rm fD}K_{\rm r}}\frac{\partial p_{\rm D}}{\partial T_{\rm D}}\Big){\rm d}A$$
$$= \int_\Gamma N_i^e \frac{\partial p_{\rm Dw}}{\partial n}{\rm d}l. \tag{9}$$

The finite element discrete equation is

$$\begin{aligned}
&K_{\rm r}A\Big(b_i^2 + c_i^2 + \frac{1}{6C_{\rm fD}K_{\rm r}\Delta T_{\rm D}} - \frac{\alpha_{2\rm D}}{6}\Big)p_i^{e,n+1}\\
&+ K_{\rm r}A\Big(b_ib_j + c_ic_j + \frac{1}{12C_{\rm fD}K_{\rm r}\Delta T_{\rm D}} - \frac{\alpha_{2\rm D}}{12}\Big)p_j^{e,n+1}\\
&+ K_{\rm r}A\Big(b_ib_k + c_ic_k + \frac{1}{12C_{\rm fD}K_{\rm r}\Delta T_{\rm D}} - \frac{\alpha_{2\rm D}}{12}\Big)p_k^{e,n+1}\\
&- \frac{L}{3}\frac{\partial p_i^{e,n+1}}{\partial n} - \frac{L}{6}\frac{\partial p_{j,k}^{e,n+1}}{\partial n}\\
=\ &\frac{A}{6C_{\rm fD}\Delta T_{\rm D}}p_i^{e,n} + \frac{A}{12C_{\rm fD}\Delta T_{\rm D}}p_j^{e,n} + \frac{A}{12C_{\rm fD}\Delta T_{\rm D}}p_k^{e,n}\\
&+ \frac{1}{3}K_{\rm r}A(\alpha_{1\rm D} - \alpha_{2\rm D}p_{\rm CD}).
\end{aligned} \tag{10}$$

When the total flux of the inner boundary equals the volume of production, i.e.,

$$\begin{aligned}
&\frac{1}{2\pi}\sum_{i=1}^{N} L_{i\rm D}\frac{\partial p_{i\rm D}^{e,n+1}}{\partial n} + \frac{1}{\Delta T_{\rm D}}p_{\rm wD}^{e,n+1}\\
&= 1 + \frac{1}{\Delta T_{\rm D}}p_{\rm wD}^{e,n},
\end{aligned} \tag{11}$$

the pressure of each point of inner boundary is

$$p_{i\rm D} = p_{\rm wD}, \tag{12}$$

where

$$\begin{cases}
A = \dfrac{1}{2}\begin{vmatrix} 1 & x_i & y_i \\ 1 & x_j & y_j \\ 1 & x_k & y_k \end{vmatrix},\\
b_i = \dfrac{1}{2A}(y_i - y_k), \quad c_i = \dfrac{1}{2A}(x_k - x_j),\\
b_j = \dfrac{1}{2A}(y_k - y_j), \quad c_j = \dfrac{1}{2A}(x_i - x_k),\\
b_k = \dfrac{1}{2A}(y_i - y_j), \quad c_k = \dfrac{1}{2A}(x_j - x_i).
\end{cases}$$

The simultaneous equations (10)–(12) are assembled by unit equations so as to solve the system equations. Then, the pressure value at the grid node (x, y) and the $(n+1)$ instant and the pressure derivative on the fracture can be obtained immediately.

2.3.2 Discrete grid for finite elements

In order to calculate the finite elements, it is necessary to discrete the research region in the coalbed by using the triangular unstructured grids within the round out-boundary.

2.3.3 Judge transformation matrix

In order to ensure the stability of the finite element solutions, the maximum spectral radius of the transformation matrix needs to be less than or equal to 1. The transformation matrix is associated with the grid, time step, and other calculated parameters. Therefore, the maximum spectral radius of the transformation matrix must be calculated at each time step, different grids, or different parameters. If the maximum spectral radius of the transformation matrix is greater than 1, the time step can be modified. The error formula of the linear interpolation for the triangular element[17] is

$$\begin{cases} |u-U| \leqslant \dfrac{3}{4}M_2h^2, \\ \left|\dfrac{\partial u}{\partial x}-\dfrac{\partial U}{\partial x}\right| \leqslant \dfrac{4M_2h}{\sin\theta}, \\ \left|\dfrac{\partial u}{\partial y}-\dfrac{\partial U}{\partial y}\right| \leqslant \dfrac{4M_2h}{\sin\theta}, \end{cases} \tag{13}$$

where u is the numerical solution, U is the real solution, M_2 is constant, h is the largest length of the triangle, and θ is the largest angle of the triangle.

Through the analysis of the error formula, we can see that large obtuse triangle is not allowed in order to ensure the convergence of the finite element solutions. The grid is generated by Gambit (see Fig. 1(a)), which can make sure that the triangle is approximate to the equilateral triangles except some small acute triangles in the fracture (see Fig. 1(b)). Moreover, the grid size is required to be large enough so as to make sure that the solutions are not sensitive to the grid.

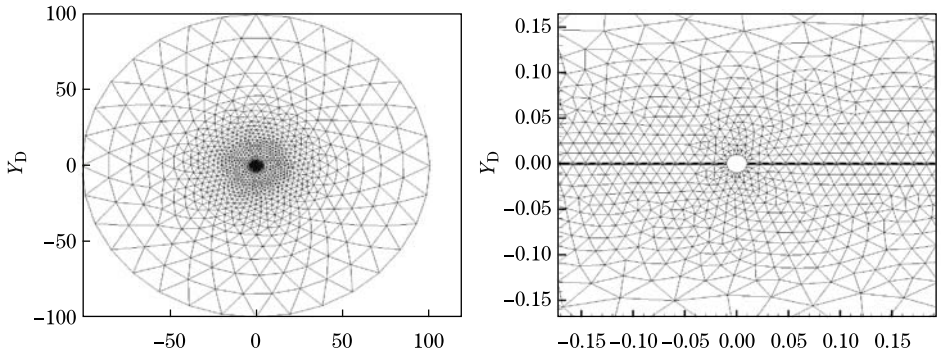

Fig. 1 Unstructured grid chart of research region in coalbed

3 Result and analysis

3.1 Well test type curve

The following parameters are taken: the dimensionless fracture storage C_{fD} is 0.001, the dimensionless fracture conductivity is 2, the dimensionless fracture width is 0.002, and the radius of the closed outer boundary is 100. The calculation results are shown in Fig. 2. The well test type curve is generally divided into 4 parts based on the characteristics in different stages. The first part is the wellbore control section line with the slope 1. The second part

indicating the finite conductivity fracture feature is the straight line with the slope 0.25. The third part is a horizontal line of 0.5 with a radial fluid flow around the wellbore. The fourth part is the straight line with the slope 1, showing the effect of the closed outer boundary.

The pressure distribution in the bed is shown in Fig. 3. The flow is the radius flow in the far field from the well bore. However, the flow forms "eye shape" nearby the fracture of the well bore, and forms ellipse shape at the place a little bit far from the well. It can be thought that the propagation speed of the pressure in the fracture is faster than that in any other region owing to its much bigger permeability.

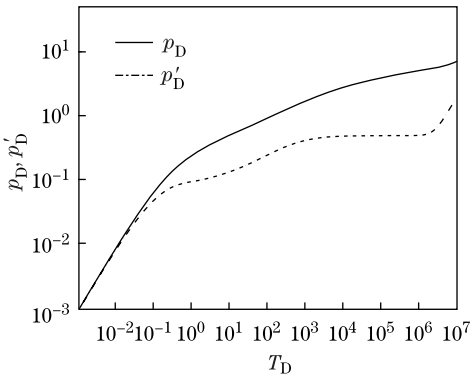

Fig. 2 Log-log type curves for fractured well with finite conductivity fracture

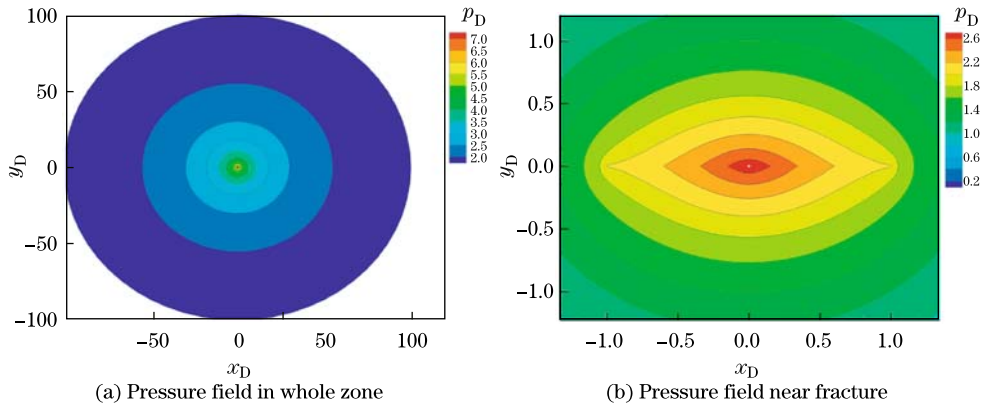

(a) Pressure field in whole zone (b) Pressure field near fracture

Fig. 3 Distributions of pressure in bed

3.2 Effects of fracture storage on type curves

Fracture storage is defined as the storage capacity of a fracture. We choose the fracture storage C_{fD} to be 0.000 1, 0.001, 0.01, and 0.1, respectively, and the fracture conductivity to be 2. The results are shown in Fig. 4. From Fig. 4, it can be seen that the smaller C_{fD} is, the shorter the storage time lasts and thus the longer the time of the linear flow in the fracture lasts. If C_{fD} becomes larger, the fracture features are not much obvious. When C_{fD} is large enough (see Curve 4 in Fig. 4), the features of the linear flow are covered by the wellbore storage.

3.3 Effects of fracture conductivity on type curves

The fracture conductivity is defined as the conductive capacity of the fracture. First, the fracture conductivities for different fractures affected on the calculating results are developed. We choose F_{CD} to be 0.1, 1, 10, and 100, respectively, C_{fD} to be 0.001, and the radius of

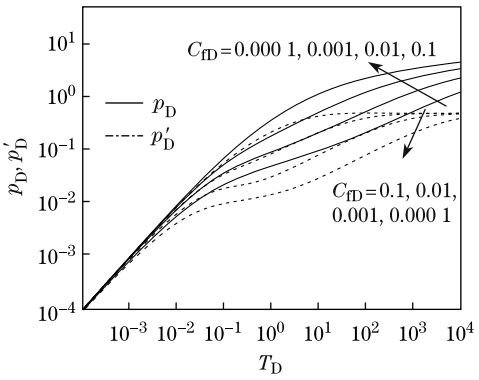

Fig. 4 Log-log type curves with different C_{fD}

the closed outer boundary to be 100. The results are shown in Fig. 5. From Fig. 5, we can see that larger fracture conductivity corresponds to lower ratio of dimensionless pressure. It means that the greater the fracture conductivity is, the lower the flow resistance of the well bottom is, and the more convenient the fracture conductivity is to produce. When the fracture conductivity is very small (see the curve corresponding to $F_{CD} = 0.1$ in Fig. 5), the fracture feature is not distinct and there is no linear section on the curve. Therefore, after reaching the storage section, the radius flow immediately comes in the wellbore. Moreover, the conductivity capacity of the fracture is very great. See the curve of $F_{CD} = 100$ in Fig. 5 for example, the fracture feature section with the slope nearly 0.5 is on the characteristic curve. However, on the distribution of pressure (see Fig. 6), there is elliptic flow in the fracture region. The pressure difference does not exist in the fracture. It is pointed out that the features mentioned above are similar to infinite conductivity. It indicates that infinite conductivity is a special case of finite conductivity. It is reasonable and natural.

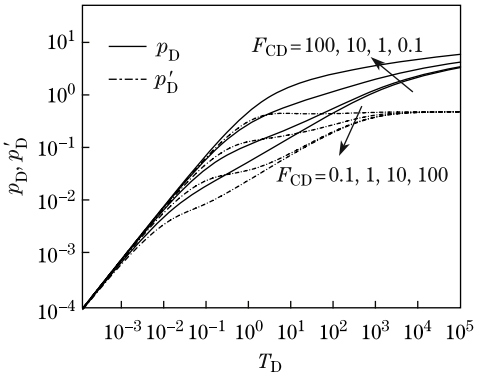

Fig. 5 Type curves with different conductivity capacities

3.4 Effects of desorption on type curves

Considering the effect of the steady desorption coefficient of the coalbed, i.e., α_{1D}, we take α_{1D} to be 0, -10^{-4}, and -2.0×10^{-4}, respectively, the unsteady desorption coefficient α_{2D} to be 0, the fracture storage of the well bore C_{fD} to be 0.001, and the radius of boundary R_{eD} to be 100. The results are shown in Fig. 7. The early section of the type curve is not affected by desorption but by the storage of the wellbore and fracture. The steady desorption strongly affects the late section of the type curve. Desorption can relieve pressure. The stronger the

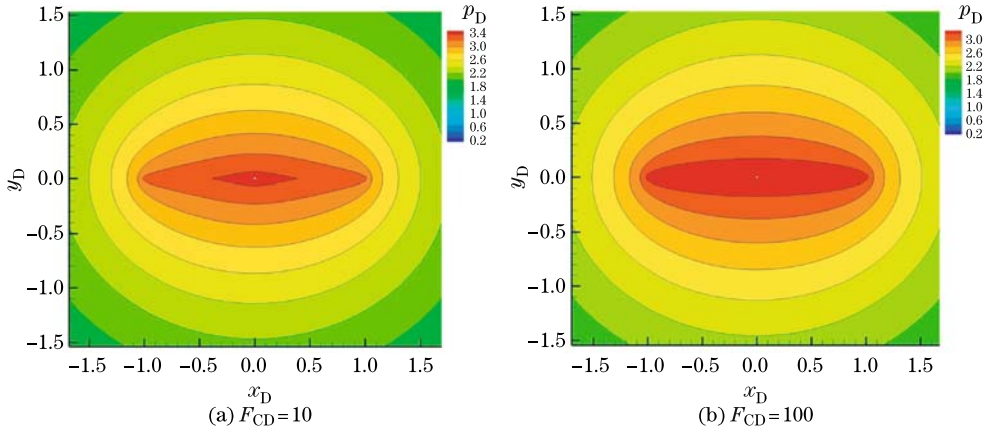

Fig. 6 Distributions of pressure field with different F_{CD}

strength of desorption is, the stronger the relieve pressure is. When the strength of desorption gets some level, the flow runs into a constant pressure boundary (see Fig. 7). The curves of the pressure derivative are going down, but those of the pressure are constant. The flow becomes stable. The desorption and production reach balance.

We examine unsteady desorption, i.e., α_{2D}, effects. We take

$$\begin{cases} \alpha_{2D} = 0, -1.0 \times 10^{-4}, -2.0 \times 10^{-4}, \\ C_{fD} = 0.01, \quad R_{eD} = 100. \end{cases}$$

As shown in Fig. 8, the early section of the curve is similar to the case of steady desorption, and it is not affected by the unsteady desorption.

As the pressure decreases in the bed unsteadily, the desorption speed of the coalbed increases, and thus the pressure decrease in the coalbed is relieved. However, because of the effect of the closed outer boundary, the pressure in the coalbed must continue to decrease, and the relevant speed of the unsteady desorption varies faster. When the desorption speed contents the production value, the pressure keeps to be constant and the pressure derivative decreases. With the effect of the unsteady desorption, the pressure in the coalbed can reach stability without any change. It is also similar to a constant pressure boundary. On the other hand, on

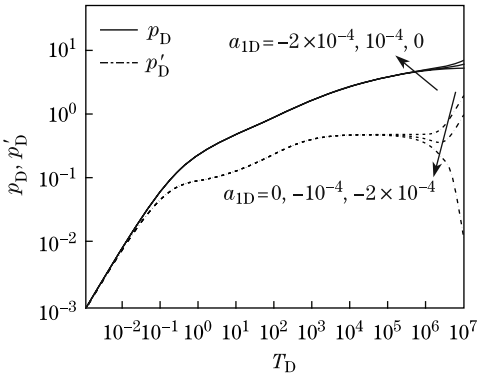

Fig. 7 Type curves for fractured well with different α_{1D}

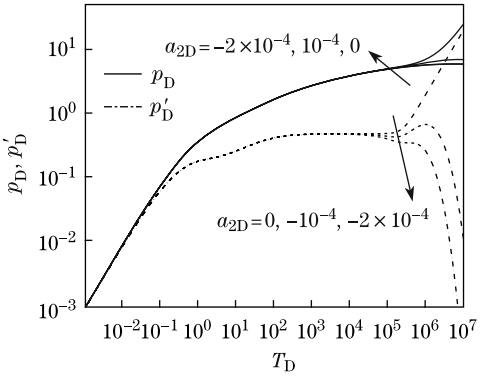

Fig. 8 Type curves for fractured well with different α_{2D}

the pressure distribution, desorption can relieve propagation of the pressure wave. When the desorption speed contents production, the propagation of the pressure wave will cease.

3.5 Effect of fracture asymmetry on type curves

Normally, the fractures are symmetric around the wellbore in sand oil reservoir, but the hydraulic fractures are asymmetric in coalbed. The asymmetric fracture effects on the curve are analyzed now. We take the fracture length ratios for both sides of the wellbore to be 1 : 1, 0.8 : 1.2, 0.6 : 1.4, 0.4 : 1.6, and 0.2 : 1.8, respectively, the fracture storage C_{fD} to be 0.001, and the radius of the closed out boundary R_{eD} to be 100. From Figs. 9 and 10, it can be seen that the more asymmetric the fractures are, the greater the dimensionless pressure is. The phenomenon can be explained by that the flow resistance in the bottom of the well is so great that it is not convenient for the fluid flow.

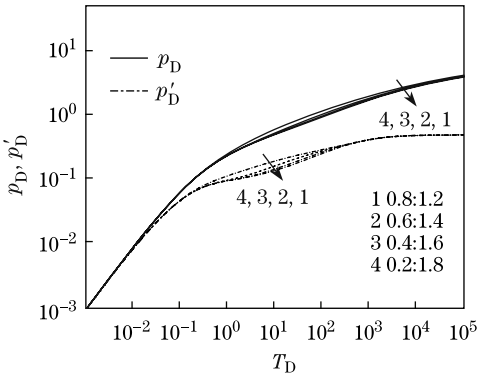

Fig. 9 Type curves for asymmetry fracture with different fracture length ratios for both sides of wellbore

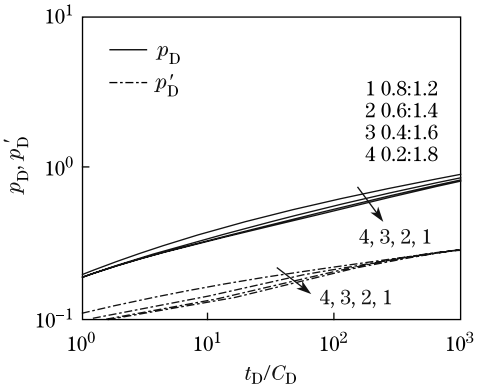

Fig. 10 Type curves for asymmetry fracture with different fracture length ratios for both sides of wellbore (part amplified)

Figure 11 shows the pressure distributions around the wellbore with different fracture length ratios for both sides of the wellbore. The speed of the pressure propagation is different for both sides because of the fracture asymmetry (see Fig. 11). The results concluded that faster pressure propagation speed corresponds to longer fracture and lower flow resistance.

4 Real case in CBM reservoir engineering

In order to verify the numerical mathematical model, a set of field well test data is used to match the type curve generated by the new model. The field well test is executed at one CBM well in the X-CBM reservoir of China in March 2011. The depth of the CBM well is 860 m. The injection rate is 3.2 m^3/d. The thickness of the coalbed is 5.6 m. The test lasts 36 hours. The results are shown in Fig. 12. From Fig. 12, we can see that the pressure changes along with the time. The solid line is the theoretical result which is calculated by the model introduced in this paper.

By matching the real test data with the well test type curve similar to Fig. 2, the parameters are obtained from an advanced well test analyzing method. The results show that the permeability of the coalbed is 0.126 mD, The fracture conductivity is 0.193 mD·m. The half-length of the fracture is 1.53 m. The fracture asymmetry equals 1.0. These results are accepted by CBM reservoir engineers.

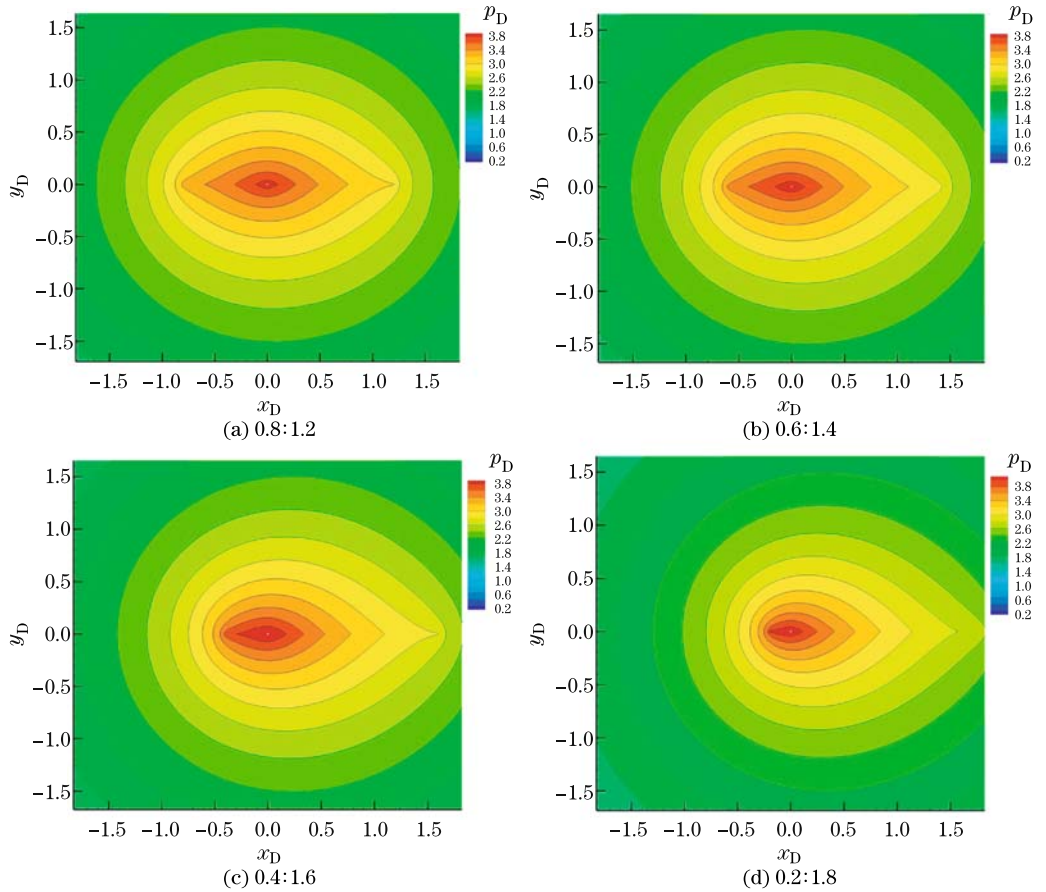

Fig. 11 Pressure distributions for asymmetry fracture with different fracture length ratios for both sides of wellbore

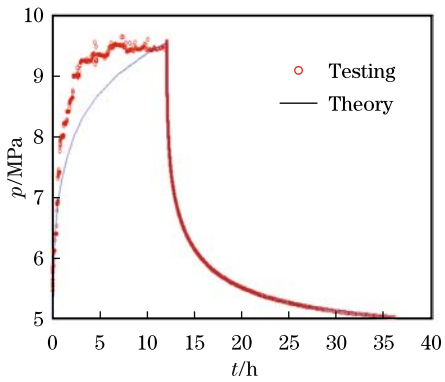

Fig. 12 Well test history sketch of pressure

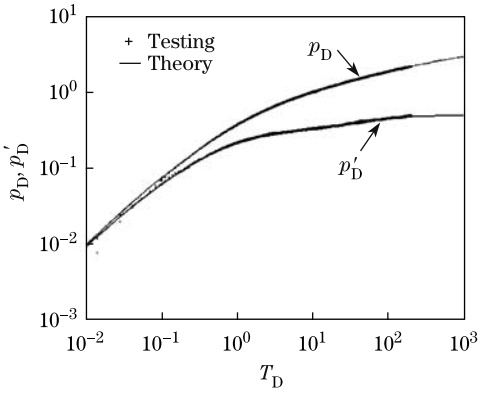

Fig. 13 Well test data matching theoretical type curve of new model

5 Conclusions

A numerical model of well tests for the well with a finite conductivity vertical hydraulic fracture in coalbed is developed in this paper by considering the fracture features of the finite

conductivity, the storage coefficient of the wellbore, the conductivity capacity of the fracture, the desorption of the coalbed, and the symmetry of the fracture. FEM is used to solve the model. The conclusions can be made as follows:

(i) There is an obvious fracture feature in the initial theoretical characteristic curve. It indicates a straight line with a slope 0.25. The pressure distribution in the coalbed indicates that the fluid flow is a radial flow far from the wellbore. However, the flow forms as an elliptic flow nearby the fracture in the early time.

(ii) Smaller combined fracture storage coefficient C_{fD} corresponds to shorter storage period and longer time for the linear flow in the fracture. When the storage coefficient C_{fD} becomes larger, the fracture features are not distinct. Therefore, the behavior of linear flow may disappear when the storage capacity is large enough.

(iii) The greater the fracture conductivity is, the smaller the flow resistance of well is, and thus the more effective the pressure is on the producing rate. The fracture feature is consistent to the infinite conductivity when the conductivity capacity of the fracture is strong enough, i.e., infinite conductivity is a special case of finite conductivity. Moreover, the fracture feature is not evident when the conductivity capacity is weak. It is difficult to see that the elliptic flow in the pressure field and its effect on the pressure is very poor.

(iv) Desorption of CBM is able to relieve pressure drop. The steady desorption which can reduce pressure decay is related to the values of the steady desorption coefficient and the region, and it is not related to the values of the pressure drop. However, the ability to relieve the pressure drop is increased with the increase in the amplitude of the pressure drop for unsteady desorption. When the desorption speed contents production, the propagation of the pressure wave will cease. It seems to reach a constant pressure boundary.

(v) The fracture asymmetry goes against the flow to in the wellbore. When the fracture asymmetry is serious, the flow resistance becomes greater.

References

[1] Gringarten, A. C., Ramey, H. J., Jr., and Raghavan, R. Unsteady-state pressure distributions created by a well with a single infinite-conductivity vertical fracture. *Society of Petroleum Engineers Journal*, **14**, 347–360 (1974)

[2] Cinco-Ley, H. and Meng, H. Z. Pressure transient analysis of wells with finite conductivity vertical fractures in double porosity reservoirs. *SPE Annual Technical Conference and Exhibition*, Houston, Texas (1988)

[3] Cinco-Ley, H. and Samaniego, F. Transient pressure analysis for fractured wells. *Journal of Petroleum Technology*, **33**, 1749–1766 (1981)

[4] Lee, S. and Brockenbrough, J. R. A new approximate analytic solution for finite-conductivity vertical fractures. *SPE Formation Evaluation*, **1**, 75–88 (1986)

[5] Riley, M. F., Brigham, W. E., and Horne, R. N. Analytic solutions for elliptical finite-conductivity fractures. *SPE Annual Technical Conference and Exhibition*, Dallas (1991)

[6] Liu, C. Q. and Yang, J. Well test analysis for finite conductivity vertical fractured well in dual-pore medium reservoir. *Well Testing and Production Technology*, **11**, 5–9 (1990)

[7] Liu, Y. W. and Liu, C. Q. Well test analysis for finite conductivity vertical fractured well in consideration of wellbore storage and skin effect. *Well Testing*, **2**, 2–10 (1993)

[8] Anbarci, K. and Ertekin, T. Pressure transient behavior of fractured wells in coalbed reservoirs. *SPE Annual Technical Conference and Exhibition*, Washington, D. C. (1992)

[9] He, Y. F. and Hang, Y. P. Transient pressure analysis for fractured well in coalbed. *Acta of Oil and Gas*, **28**, 113–117 (2006)

[10] Liu, Y. W., Zhang, D. W., Chen, H. X., and Gong, X. Numerical study on coalbed methane transient seepage flow with multiwells (in Chinese). *Journal of Rock Mechanics and Engineering*, **24**, 1679–1685 (2005)

[11] Anbarci, K. and Ertekin, T. Comprehensive study of pressure transient analysis with sorption phenomena for single-phase gas flow in coal seams. *SPE Annual Technical Conference and Exhibition*, New Orleans, Louisiana (1990)

[12] Ertekin, T. and Sung, W. Pressure transient analysis of coal seams in the presence of multi-mechanistic flow and sorption phenomena. *The SPE Gas Technology Symposium*, Dallas, Texas (1989)

[13] Langmuir, I. The constitution and fundamental properties of solids and liquids, part 1: solid. *Journal of American Chemical Society*, **38**, 2221–2295 (1916)

[14] Ouyang, W. P. and Liu, Y. W. Numerical well test model for CBM infinite conductivity vertical fracture well. *Well Testing*, **19**, 53–56 (2010)

[15] Liu, Y. W., Su, Z. L., Fang, H. B., and Zhang, J. F. Review on CBM desorption/adsorption mechanism. *Well Testing*, **19**, 37–44 (2010)

[16] Aminian, K. and Ameri, S. Predicting production performance of CBM reservoirs. *Journal of Natural Gas Science and Engineering*, **1**, 25–30 (2009)

[17] Feng, K. Finite element method (II). *Mathematics in Practice and Theory*, **5**, 42–54 (1975)